

Facile and Mass-Productible Fabrication of One-Dimensional Ag Nanoparticle Arrays

Junichi Nishijo, Osamu Oishi, Ken Judai, and Nobuyuki Nishi*

Department of Electronic Structure,
Institute for Molecular Science, 38 Nishigo-naka,
Myodaiji, Okazaki, 444-8585 Japan

Received June 24, 2007

Revised Manuscript Received July 26, 2007

There has been an extensive effort to construct one-dimensional (1D) metal-nanoparticle (NP) arrays because their exceptional magnetic, electronic, optical, and catalytic properties are expected to be appropriate for nanoscale devices.¹ As compared with two- or three-dimensional NP arrays, assembling 1D NP arrays is much more challenging to achieve because of the isotropic structure and the nondirectional interaction of NPs, which makes NPs aggregate three-dimensionally in a solution or two-dimensionally on a surface. To circumvent the difficulty in constructing 1D structure from isotropic NPs, most previous studies have focused on assembling NPs on 1D templates such as DNA, nanotubes, 1D structure of substrate, etc.² Although the existing template techniques have brought a lot of impressive results, it is still fascinating to develop new preparation methods of 1D NP arrays because more facile production methods in large quantity are desirable in applications.

In this paper, we demonstrate a new facile fabrication method for diameter-controlled 1D Ag NP arrays. To create 1D NP arrays, we employed the decomposition of nanowires consisting of metal cations and reducing ligands. Metal cations in a nanowire are reduced by the ligands and form metal NPs during the decomposition process caused by heating or UV irradiation. This decomposition method has the following two advantages: First, the decomposition method automatically gives 1D NP arrays without any templates because of the wire shape of the starting material. This feature greatly simplifies the assembling process and enables the large-scale production. Second, because each part of a nanowire is essentially homogeneous, it is hard to expect any part to be excessively or insufficiently accumulated in a 1D NP array. In this work, we use silver phenylacetylide ($[\text{Ag}-\text{C}\equiv\text{C}-\text{Ph}]$) as a raw material. By using the complex,

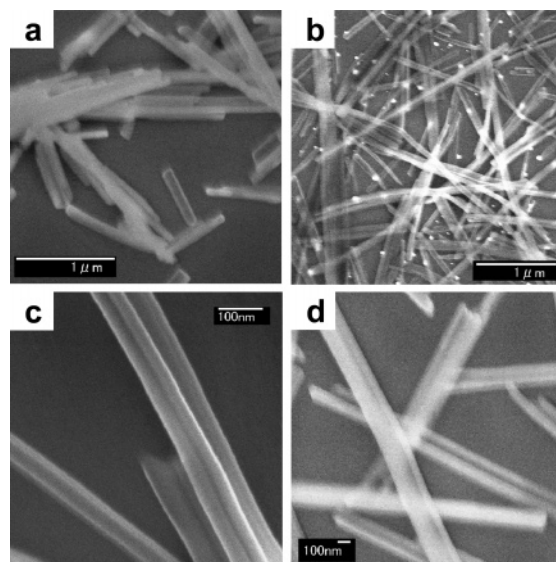


Figure 1. SEM images of $[\text{Ag}-\text{C}\equiv\text{C}-\text{Ph}]$. (a) AS, (b, c) wire/EtOH bundles, (d) wire/1-BuOH bundles.

we expect thin wire-shaped crystals because of their highly anisotropic crystal structure,³ whereas the strong reducing power of ethynyl anion allows us to convert the raw material into the assembly of Ag NPs under mild conditions. Furthermore, phenylacetylene molecules will polymerize and form an organic matrix surrounding Ag NPs in the decomposition process, which seems to be suitable for keeping the wire shape and protecting the Ag NPs from oxidation.⁴

$[\text{Ag}-\text{C}\equiv\text{C}-\text{Ph}]$ and $[\text{Me}_3\text{P}-\text{Ag}-\text{C}\equiv\text{C}-\text{Ph}]$ were prepared according to the literature.⁵ Though it is well-recognized that $[\text{Ag}-\text{C}\equiv\text{C}-\text{Ph}]$ cannot be recrystallized because of its poor solubility, we succeeded in it by using the ligand dissociation of $[\text{Me}_3\text{P}-\text{Ag}-\text{C}\equiv\text{C}-\text{Ph}]$. We will abbreviate as-prepared and recrystallized $[\text{Ag}-\text{C}\equiv\text{C}-\text{Ph}]$ from a solvent as “AS” and “wire/solvent”, respectively, in this article. The scanning electron microscope (SEM) images of AS and wire/solvent are shown in Figure 1. In contrast to the rodlike crystals of AS, recrystallized samples are obtained as long nanowires. As generally known, the crystal size obtained by recrystallization largely depends on the recrystallization conditions, which suggests that we can control the nanowire diameter by changing the recrystallization solvent. Indeed, the diameter of the nanowires recrystallized from one solvent clearly differs from that from other solvent. For example, the diameter of wire/EtOH, whose recrystallization process is fast, is 39 ± 11 nm, whereas that of wire/1-BuOH, whose recrystallization process is slow, is 94 ± 12 nm, as demonstrated in images c and d in Figure 1. The

* Corresponding author. E-mail: nishi@ims.ac.jp.

- (1) (a) Hu, M.-S.; Chen, H.-L.; Shen, C.-H.; Hong, L.-S.; Huang, B.-R.; Chen, K.-H.; Chen, L.-C. *Nat. Mater.* **2006**, *5*, 102. (b) Grzelczak, M.; Correa-Duarte, M. A.; Salgueiriño-Maceira, V.; Giersig, M.; Diaz, R.; Liz-Marzán, L. M. *Adv. Mater.* **2006**, *18*, 415. (c) Brongersma, M. L.; Hartman, J. W.; Atwater, H. A. *Phys. Rev. B* **2000**, *62*, R16356. (d) Maier, S. A.; Kik, P. G.; Atwater, H. A.; Meltzer, S.; Harel, E.; Koel, B. E.; Requicha, A. A. G. *Nat. Mater.* **2003**, *2*, 229. (e) Wei, Q.-H.; Su, K.-H.; Durant, S.; Zhang, X. *Nano Lett.* **2004**, *4*, 1067. (f) Hunyadi, S. E.; Murphy, C. J. *J. Phys. Chem. B* **2006**, *110*, 7226.
- (2) (a) Deng, Z. D.; Tian, Y.; Lee, S.-H.; Ribbe, A. E.; Mao, C. *Angew. Chem., Int. Ed.* **2005**, *44*, 3582. (b) Correa-Duarte, M. A.; Pérez-Juste, J.; Sánchez-Iglesias, A.; Giersig, M.; Liz-Marzán, L. *Angew. Chem., Int. Ed.* **2005**, *44*, 4375. (c) Cheng, J. Y.; Zhang, F.; Chuang, V. P.; Mayes A. M.; Ross, C. A. *Nano Lett.* **2006**, *6*, 2099. (d) Huang, J.; Tao, A. R.; Connor, S.; He, R.; Yang, P. *Nano Lett.* **2006**, *6*, 524.

- (3) Chui, S. S. Y.; Ng, M. F. Y.; Che, C.-M. *Chem.-Eur. J.* **2005**, *11*, 1739.
- (4) (a) Nishijo, J.; Okabe, C.; Oishi, O.; Nishi, N. *Carbon* **2006**, *44*, 2943. (b) Judai, K.; Nishijo, J.; Nishi, N. *Adv. Mater.* **2006**, *18*, 2842. (c) Nishi, N.; Nishijo, J.; Oishi, O. *Eur. Phys. J. D* **2007**, *43*, 287.
- (5) (a) Teo, B. K.; Xu, Y. H.; Zhong, B. Y.; He, Y. K.; Chen, H. Y.; Qian, W.; Deng, Y. J.; Zou, Y. H. *Inorg. Chem.* **2001**, *40*, 6794. (b) Schuster, O.; Monkowius, U.; Schmidbaur, H.; Ray, R. S.; Krüger, S.; Rösch, N. *Organometallics* **2006**, *25*, 1004.

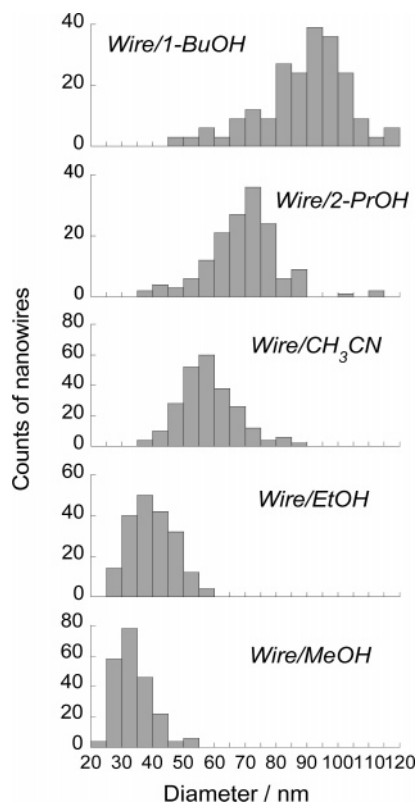


Figure 2. Histogram of diameter distributions for wire/solvent derived from SEM images.

diameter distributions of the nanowires recrystallized from different solvents are summarized in Figure 2. The histogram clearly indicates the controllability of the nanowire diameter in the range of 30–100 nm. Roughly speaking, a faster PMe_3 dissociation rate in a higher-polarity solvent leads to thinner $[\text{Ag}-\text{C}\equiv\text{C}-\text{Ph}]$ nanowires, whereas a slow crystal growth in a lower-polarity solvent brings thicker nanowires. The lengths of wire/ROH are approximately in proportion to their diameters with an aspect ratio of ca. 30–40, whereas that of wire/ CH_3CN is obviously longer (aspect ratio > 100) and sometimes reaches 100 μm . This difference probably originated from the coordination of acetonitrile molecules to silver atoms during the recrystallization process, but the detail remains unclear. In both cases, the nanowire lengths can be shortened by stirring, whereas the diameters show only small changes.

The nanowires can be rapidly converted into Ag NP arrays embedded in polymerized phenylacetylene matrices by UV irradiation. Figure 3a shows the UV/vis spectrum of wire/EtOH before and after UV irradiation. The broad absorption peak at around 485 nm appears after 15 min irradiation. This strong absorption is attributed to the surface plasmon resonance band of Ag NPs. The absorption maximum wavelength of 485 nm is somewhat longer than that of typical Ag NPs at around 400 nm.⁶ This red shift is most likely due to the short distance between Ag NPs (see later in the text). It is known that the dipole–dipole interaction between metal

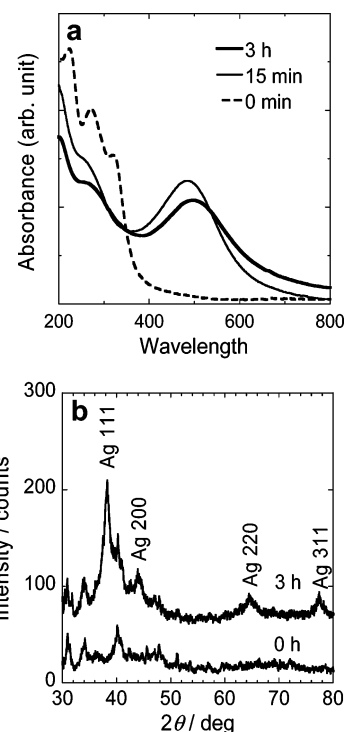


Figure 3. (a) UV/vis spectrum of wire/EtOH for different UV irradiation times: 0 min (dashed line), 15 min (solid line), and 3 h (bold line). (b) XRD patterns of wire/EtOH before and after 3 h of UV irradiation.

NPs causes the red shift of surface plasmon resonance.⁷ In addition, the high dielectric constant of the matrix is thought to lower the plasmon frequency.⁸ The matrix of the decomposed nanowires mainly consists of sp^2 -bonded carbons formed by the polymerization of phenylacetylene, whose π -system will show a high dielectric constant. The absorption peak is slightly red-shifted and weakened by longer UV irradiation time. These variations are due to the increase in the Ag particle size, which weakens the surface plasmon absorption and lowers the surface plasmon frequency.⁹ The plasmon absorption of the 15 min UV-irradiated nanowires is as strong as that of 3 h, suggesting that most of the $[\text{Ag}-\text{C}\equiv\text{C}-\text{Ph}]$ complex is decomposed into Ag NPs in tens of minutes.

The formation of Ag NPs is also evidenced by powder X-ray diffraction (XRD) patterns. Figure 3b shows the XRD patterns of wire/EtOH before and after 3 h of UV irradiation. Because the penetration depth of X-ray is much longer than that of UV light, the pattern after UV irradiation contains not only the diffraction peaks from the decomposed material but also those from the raw material. Four new peaks at $2\theta = 38.2, 44.1, 64.6,$ and 77.4° are found after UV irradiation, which are assigned to the (111), (200), (220), and (311) planes of fcc-silver, respectively. The Ag particle size of ca. 5 nm is estimated from the peak widths and Scherrer equation, but it should be noted that this value is probably

(6) (a) Mohan, Y. M.; Premkumar, T.; Lee, K.; Geckeler, K. E. *Macromol. Rapid Commun.* **2006**, *27*, 1346. (b) Eustis, S.; Krylova, G.; Eremenko, A.; Sminova, N.; Schill, A. W.; El-Sayed, M. *Photochem. Photobiol. Sci.* **2005**, *4*, 154. (c) Hu, J.; Cai, W.; Zeng, H.; Li, C.; Sun, F. *J. Phys.: Condens. Matter* **2006**, *18*, 5415.

(7) (a) Rast, L.; Stanishevsky, A. *Appl. Phys. Lett.* **2005**, *87*, 223118. (b) Tamaru, H.; Kuwata, H.; Miyazaki, T.; Miyano, K. *Appl. Phys. Lett.* **2002**, *80*, 1826. (c) Podlipensky, A.; Abdolvand, A.; Seifert, G.; Gaener, H. *Appl. Phys. A* **2005**, *80*, 1647. (d) Wang, J.; Lau, W. M.; Li, Q. *J. Appl. Phys.* **2005**, *97*, 114303. (e) Sakata, J. K.; Dwoskin, A. D.; Vigorita, J. L.; Spain, E. M. *J. Phys. Chem. B* **2005**, *109*, 138. (8) Mie, G. *Ann. Phys.* **1908**, *25*, 377. (9) Germain, V.; Brioude, A.; Ingert, D.; Pileni, M. P. *J. Chem. Phys.* **2005**, *122*, 124707.

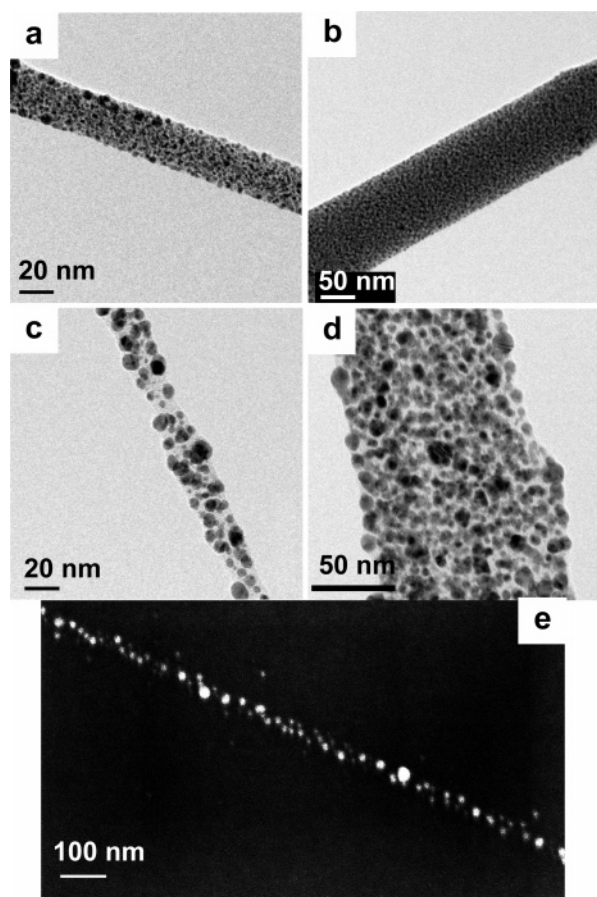


Figure 4. (a–d) TEM images of UV-irradiated silver phenylacetylide nanowires: (a) wire/EtOH, 15 min of irradiation; (b) wire/1-BuOH, 15 min of irradiation; (c) wire/EtOH, 3 h of irradiation; (d) wire/1-BuOH, 3 h of irradiation. (e) SEM image of decomposed wire/EtOH. Ag NPs are fixed on a Si substrate by heating after UV irradiation (see text).

affected by the limited penetration depth of UV light, bringing smaller particles at the inner part of the sample tablet.

The transmission electron microscope (TEM) images of UV-irradiated nanowires are shown in Figure 4. It is obvious that a nanowire is converted into an assembly of Ag NPs after irradiation, whereas the wire shape of an assembly is kept thanks to the matrix consisting of polymerized phenylacetylene. As a natural consequence of using the decomposition method, the decomposed nanowire consists of closely packed Ag NPs without any excessively or insufficiently accumulated part. The particle size is independent of wire diameter and increases with the irradiation time; for example, the Ag NP diameters are 2.3 ± 0.6 and 5.8 ± 2.1 nm for 15 min and 3 h of irradiation, respectively. This is consistent

with the red shift of the surface plasmon resonance for longer irradiation. Interparticle distances are approximately 1 nm for 15 min and 3 nm for 3 h of irradiation, respectively.

The heating also brings the decomposition of silver phenylacetylide. For example, the heat treatment of the nanowires at 110 °C for 3 h gives 1D arrays of Ag NPs with the diameter of 2.4 ± 0.7 nm, the value of which is roughly the same as that of 15 min UV irradiated material. In contrast to low-temperature decompositions, a higher heat-treatment temperature such as 150 °C is not suitable for creating a 1D NP array. Because the degree of polymerization of phenylacetylene is low in the pyrolyzed sample, the organic part of the decomposed nanowire is melted and evaporated at higher temperature, where Ag NPs are spread on a substrate and no longer keep thin 1D structure. However, this melting and evaporation process of the organic matrix allow us to fix NPs on a substrate as follows; First, wire/solvent deposited on a substrate is decomposed by UV irradiation for 1 h. This process not only decomposes the nanowires but also promotes the polymerization of phenylacetylene. The nanowires are then heated at 150 °C under vacuum conditions, where most of the organic matrix is removed by evaporation. During the evaporation process, a small amount of highly polymerized phenylacetylene keeps Ag NPs one-dimensional like a net, resulting in 1D Ag NP arrays fixed on a substrate as shown in Figure 4e.

In summary, we have developed the new method for constructing 1D Ag NP arrays via decomposition of silver phenylacetylide nanowires. Using this method, we can easily construct 1D Ag NP arrays in large scale without any templates. The diameter of arrays can be controlled by changing the recrystallization solvent, whereas the particle diameter is roughly controlled by UV irradiation time. The Ag NPs can be fixed on a substrate by heating, where the 1D alignment of NPs is kept during the evaporation process of the organic matrix.

Acknowledgment. This work is supported by Grants-in-Aid for Scientific Research and “Nanotechnology Support Project” of the Ministry of Education, Culture, Sports, Science and Technology (MEXT), Japan.

Supporting Information Available: Experimental details, SEM images of wire/solvent, size distributions of the photo- and thermally converted Ag NPs, and change in resistivity with UV irradiation time (PDF). This material is available free of charge via the Internet at <http://pubs.acs.org>.

CM071688I